JOURNAL OF SOLID STATE CHEMISTRY 63, 267–277 (1986)

Structural Consequences of the Coupled Substitution of Eu,S in Calcium Sulfoapatite

P. R. SUITCH,* A. TAITAI,† J. L. LACOUT,† AND R. A. YOUNG*

School of Physics, Georgia Institute of Technology, Atlanta, Georgia 30332; and †Laboratoire de Physico–Chimie des Solids, U.A. CNRS 445, ENSCT, INP 38 rue des 36 Ponts, 31400 Toulouse, France

Received August 14, 1985; in revised form November 15, 1985

Substitution of (Eu,S) for calcium in calcium sulfoapatite in a high-temperature solid state reaction produced brown powders in the continuous series $Ca_{10-x}Eu_x(PO_4)_6S_{1+x/2}$ with space group $P6_3$ for x from zero to at least 1.3. Rietveld refinements (RR) with powder X-ray diffraction data showed that the Eu^{3+} substituted only at the Ca(2) sites and that the S^{2-} occurs equally at 0,0,0.47 and 0,0,0.97, irrespective of the quantity present. RR in $P3$ showed no further ordering for either the S^{2-} or Eu^{3+} in the apatite structure. The progressive incorporation of Eu^{3+} produced changes in the Ca–O distances around both Ca sites which can be visualized as a combined rotation and scissoring of the PO_4^{3-} group. Substitution in the ratio of $(2Eu^{3+} + S^{2-})$ for 2 Ca^{2+} in the structure was confirmed by the site occupancies obtained in RR's and by the applicability of Vegard's law to the substitution. The RR's were carried out with the constraints that the PO_4^{3-} group was stoichiometric and that each of the Ca(2) sites were filled with either Eu^{3+} or Ca^{2+}. The final R_{wp} and R_B were ~0.16 and 0.03, respectively. For $x = 0$, $a = 9.4560(4)$ and $c = 6.8409(4)$ Å.

Introduction

The immediate purpose of this study was to determine the normal crystal structural location and effects of S^{2-} ions in a calcium apatite, the location(s) of Eu^{3+} progressively substituted for Ca^{2+}, the location of additional S^{2-} ions introduced to encourage charge balance and whether stoichiometry was maintained, and how the positions of already-present ions are affected by the progressive addition of these two ions. These questions are of direct interest in the mining and phosphor lighting industries, as discussed below. The questions of structural location and role of S^{2-} is of some dental research interest because human tooth enamel (TE) contains ~200 ppm S^{2-} (*1*) and essentially nothing is known in detail about its structural location nor about the local structural distortions it causes which could provide a mechanism for an active role in the health or disease of TE.

An understanding of the substitution of trivalent rare-earth apatites for calcium is important in the use of rare earth apatites for the production of lasers with high-efficiency and low-generation threshold (*2, 3*). This mechanism is also important to the mining industry since apatites are considered to be economic rare-earth concentrators only when the rare-earth element is in the particular crystallographic site Ca(2) (*4*).

The calcium phosphate apatites, $Ca_{10}(PO_4)_6X_2$ ($X = OH^-$, F^-, Cl^-, $\frac{1}{2}CO_3^{2-}$,

0022-4596/86 $3.00

$\frac{1}{2}O^{2-}$, $\frac{1}{2}S^{2-}$ . . .), are most frequently found to be crystallized in the hexagonal crystal system with a space group of $P6_3/m$, although lower symmetry forms also occur under appropriate conditions (*5–10*). In this structure, the *X*-ions occur in columns (or long chains) surrounded by O^{2-} and Ca^{2+} ions. The surrounding ions are said to form a channel (or tunnel) parallel to *c* in which the *X*-ions occur. The unit cell setting is usually chosen so that the channel is located at $x = y = 0$.

In the $P6_3/m$ structure the Ca^{2+} ions occur in two different crystallographic sites, Ca(1) and Ca(2). The Ca(2) ions form two oppositely oriented triangles per unit cell, perpendicular to and centered on the *X*-ion channels. One is at level $z = \frac{1}{4}$ and the other at $z = \frac{3}{4}$. The Ca(2) ions are coordinated by six oxygen ions and one *X*-ion. The Ca(1) ions also occur in columns but at $x = \frac{1}{3}$, $y = \frac{2}{3}$, and $x = \frac{2}{3}$, $y = \frac{1}{3}$, not near the *X*-ion channel. They are coordinated by nine O^{2-} ions, visualized as being at the vertices of a polyhedron. For further details of the hydroxyapatite structure see, for example, (*11*) and references therein. The Ca(1) site is the smaller of the two sites and thus one would expect that ions larger than Ca^{2+} (0.99 Å) would substitute primarily in the Ca(2) site while smaller substitutional ions would preferentially substitute for Ca(1) (*12*). This atomic ordering in the Ca(1) site has been observed for Mn^{2+} (0.80 Å) in calcium phosphate fluorapatite (*10*) while ordering in the Ca(2) site (up to 10 at%) has been demonstrated for most rare-earth trivalent ions in calcium (silicate, phosphate) fluorapatite (*13*).

Materials and Methods

The series of apatite specimens used in this study were ideally represented by $Ca_{10-x}Eu_x(PO_4)_6S_{1+x/2}$. A systematic study of these compositions has been carried out by Taitai (*14*). The sulfoapatites were prepared by exposing calcium europium oxyapatites to sulfur vapor at high temperatures. The oxyapatites were prepared according to a method described by Taitai *et al.* (*15*) which consists of calcining (at 1350°C in air) a mixture of anhydrous calcium phosphate, calcium carbonate, and europium oxide in proportions such that the atomic ratio (Eu + Ca)/P remains fixed at 1.67.

These samples, held under vacuum at 900°C for 10 hr, were calcined repeatedly until a single-phase calcium–europium oxyapatite was obtained as shown by X-ray diffraction and IR spectroscopy (e.g., 3570-cm^{-1} band progressively disappeared). The samples were next maintained at 900°C for 10 hr in an atmosphere of sulfur vapor (500 Torr) and then allowed to cool to room temperature in an atmosphere of helium. The brown powders that were obtained from this synthesis were determined by X-ray diffraction analysis with the Rietveld method to be single phase and with wet chemical analysis to have the above chemical formula with *x* values as shown in Table II. Chemical analyses of these compounds made before and after treatment with the sulfur vapor showed that there was no loss of phosphorous in the course of the treatments. Acid dissolution produced no evidence of precipitation of colloidal sulfur, such as would be expected from residual traces of polysulfur S_x^{2-}, and the evolution of H_2S gas confirmed the presence of sulfur ions, S^{2-}.

The existence of an upper solubility limit of sulfur was determined in a separate preparation in which an attempt was made to incorporate two Eu^{3+} per cell, which led to the formation of Eu_2O_2S as a second phase. This limit is ~1.8 S^{2-} per cell (*14*). It is reasonable that there should be a limit since it is probably sterically impossible to incorporate more than this amount of S^{2-} in the channels; the radius of the S^{2-} ion (1.84 Å) exceeds *c*/4 (<1.62 Å). A similarly steri-

cally imposed limit for Br, I, and Cl in cadmium apatites has been the subject of a single crystal X-ray diffraction study (*16, 17*).

Two independent sets of powder X-ray diffraction data (identified by PS numbers) were collected from each of the four sulfoapatite samples with crystal monochromated Cu$K\alpha$ radiation (λ = 1.5405 and 1.5443 Å) and a θ–2θ diffractometer operating in the step scan mode at 60 sec per 0.025° step. Structure refinements were carried out from these X-ray data with the Rietveld method (*18, 19*) and a locally written program (DBW 3.2 (*20*)) which implemented the pseudo-Voigt profile in the refinements. To determine whether or not there was any preferential ordering of the europium or sulfur ions in the apatite, structure refinements were conducted in space groups $P6_3/m$, $P6_3$, and $P3$.

The amounts of Eu^{3+} and S^{2-} in the structure were determined directly by refinement of the site occupancy factors. The site occupancy factors for Eu^{3+} and Ca^{2+} ions at the same site were refined simultaneously under the constraint that all of the calcium sites were occupied either by Ca^{2+} or by Eu^{3+} and that the six PO_4 groups were stoichiometric in the apatite structure. The scattering factors were those in Volume 4 of the International Tables for Crystallography (*21*) with the exception that the scattering factor for the isoelectronic Cl^- was used for S^{2-}. Other parameters that were refined included the lattice parameters, atomic position parameters, 2θ zero-point, reflection profile breadth, background, asymmetry, and preferred orientation parameters. The thermal motions for the atoms in the sulfoapatite structure were modeled by the anisotropic temperature factors determined for chlorapatite (*11*) with the refinement of an overall temperature factor to adjust for any overall differences (i.e., the differences in thermal motion between Cl^{1-} and S^{2-}, and between Ca^{2+} and Eu^{3+}). The final atomic positions were then used to calculate interatomic distances and angles with the well-known program ORFFE (*22*) so that the atomic scale effects of the introduction of Eu^{3+} and S^{2-} into the apatite structure could be better put in view.

Results

The S^{2-} per unit cell shown under "chemical analysis" in Table I was calculated from the amount of sulfur found in the specimen and the assumption of stoichiometry in (Eu + Ca) and P. These values are inferior to those expected from the proportions of the reactants used. These differences may be attributed in part to the precision of the analyses of sulfur (5%), but also to incomplete substitution of sulfur for O^{2-} ions initially present in the oxyapatite. The chemical analysis results indicate that the sulfoapatites can therefore contain, in very small amounts, however (between 0.01 and 0.09 atoms per unit cell), some O^{2-} ions.

Refinements in space group $P6_3/m$ indicated that the substitution of Eu^{3+} for Ca^{2+} occurred exclusively at the Ca(2) site, as previous authors had noted (*12*), while the S^{2-} occurred near 0,0,0.47 and symmetry-related crystallographic positions. Refinements in space group $P6_3$ showed that the mirror plane was not present, e.g., S^{2-} occurred at 0,0,0.47 but not at the mirror-related position of 0,0,0.53. Since there were less than two S^{2-} ions per cell in all cases,

TABLE I

AMOUNT OF Eu^{3+} AND S^{2-} PER UNIT CELL IN VARIOUS SULFOAPATITES

	Average from Rietveld refinements		S from chemical analysis[a]	
Sample	Eu	S	Specimens	Reactants
Y-220	—	0.85(8)	0.99	1.00
Y-249	0.35(4)	1.13(12)	1.20	1.25
Y-247	0.88(3)	1.36(4)	1.41	1.50
Y-245	1.29(9)	1.57(6)	1.70	1.75

[a] Estimated error 5%.

TABLE II

ATOMIC PARAMETERS FOR $(Ca_{10-x}Eu_x)(PO_4)_6S_{1+x/2}$

Specimen	PS No.	a (Å)	c (Å)	O(1) x	O(1) y	O(1) z	O(1) N	O(2) x	O(2) y	O(2) z	O(2) N
Y-220	720	9.4554(2)	6.8405(2)	0.3266(10)	0.4852(10)	0.2640(38)	6.0	0.5841(11)	0.4724(11)	0.3061(27)	6.0
	730	9.4561(2)	6.8411(1)	0.3253(10)	0.4841(10)	0.2758(22)	6.0	0.5820(10)	0.4748(13)	0.3106(20)	6.0
Y-249	847	9.5112(5)	6.8030(4)	0.3332(16)	0.4874(18)	0.2832(49)	6.0	0.5882(20)	0.4708(20)	0.2971(41)	6.0
	854	9.5112(4)	6.8025(3)	0.3369(16)	0.4927(17)	0.2470(63)	6.0	0.5803(19)	0.4671(19)	0.2931(39)	6.0
Y-247	853	9.5989(2)	6.7424(2)	0.3387(16)	0.4850(17)	0.2590(68)	6.0	0.5922(18)	0.4766(18)	0.2755(49)	6.0
	845	9.5977(3)	6.7416(2)	0.3437(18)	0.4885(17)	0.2496(97)	6.0	0.5935(20)	0.4660(19)	0.2797(47)	6.0
Y-245	846	9.6285(2)	6.7325(2)	0.3455(15)	0.4909(14)	0.2406(63)	6.0	0.5928(16)	0.4658(18)	0.2683(62)	6.0
	871	9.6306(3)	6.7329(2)	0.3452(18)	0.4937(17)	0.2372(54)	6.0	0.5940(17)	0.4655(18)	0.2794(41)	6.0

Specimen	PS No.	O(3a) x	O(3a) y	O(3a) z	O(3a) N	O(3b) x	O(3b) y	O(3b) z	O(3b) N
Y-220	720	0.3848(12)	0.2853(14)	0.0680(25)	6.0	−0.3080(16)	−0.2373(17)	−0.0789(17)	6.0
	730	0.3876(12)	0.2889(13)	0.0644(21)	6.0	−0.3153(16)	−0.2414(16)	−0.0703(18)	6.0
Y-249	847	0.3828(23)	0.2745(25)	0.0653(39)	6.0	−0.3079(26)	−0.2500(28)	−0.0817(27)	6.0
	854	0.3825(23)	0.2801(29)	0.0501(36)	6.0	−0.3204(27)	−0.2553(29)	−0.0861(27)	6.0
Y-247	853	0.3681(39)	0.2704(36)	0.0502(43)	6.0	−0.3386(39)	−0.2694(36)	−0.0801(36)	6.0
	845	0.3701(50)	0.2682(42)	0.0622(49)	6.0	−0.3409(48)	−0.2685(42)	−0.0712(47)	6.0
Y-245	846	0.3591(59)	0.2726(62)	0.0520(63)	6.0	−0.3531(55)	−0.2691(64)	−0.0780(57)	6.0
	871	0.3496(45)	0.2699(53)	0.0821(68)	6.0	−0.3687(45)	0.2776(52)	−0.0573(67)	6.0

Specimen	PS No.	P x	P y	P z	P N	Ca(1a) x	Ca(1a) y	Ca(1a) z	Ca(1a) N	Ca(1b) x	Ca(1b) y	Ca(1b) z	Ca(1b) N
Y-220	720	0.3968(5)	0.3720(5)	0.2441(20)	6.0	0.3333	0.6667	0.0223(19)	2.28(4)	0.6667	0.3333	0.0096(21)	1.68(4)
	730	0.3996(4)	0.3724(4)	0.2540(14)	6.0	0.3333	0.6667	0.0233(12)	2.12(4)	0.6667	0.3333	0.0103(14)	1.75(4)
Y-249	847	0.4034(9)	0.3761(9)	0.2406(39)	6.0	0.3333	0.6667	0.0142(39)	1.88(4)	0.6667	0.3333	−0.0014(37)	2.11(5)
	854	0.4049(8)	0.3782(8)	0.2418(30)	6.0	0.3333	0.6667	0.0124(36)	2.22(6)	0.6667	0.3333	−0.0039(43)	1.76(6)
Y-247	853	0.4090(8)	0.3783(8)	0.2406(34)	6.0	0.3333	0.6667	−0.0005(34)	2.09(12)	0.6667	0.3333	−0.0136(31)	2.03(13)
	845	0.4096(9)	0.3777(9)	0.2404(38)	6.0	0.3333	0.6667	−0.0054(38)	1.93(12)	0.6667	0.3333	−0.0097(35)	2.14(14)
Y-245	846	0.4112(8)	0.3794(8)	0.2570(36)	6.0	0.3333	0.6667	0.0058(36)	2.16(7)	0.6667	0.3333	−0.0040(39)	1.89(6)
	871	0.4122(7)	0.3798(6)	0.2454(33)	6.0	0.3333	0.6667	0.0109(36)	1.99(13)	0.6667	0.3333	−0.0008(42)	1.91(13)

Specimen	PS No.	Eu(2) x	Eu(2) y	Eu(2) z	Eu(2) N	Ca(2) x	Ca(2) y	Ca(2) z	Ca(2) N	S x	S y	S z	S N
Y-220	720		—[a]			0.2459(4)	−0.0110(5)	0.2500	6.00	0.0000	0.0000	0.4846(40)	0.95(2)
	730		—[a]			0.2453(3)	−0.0117(4)	0.2500	6.00	0.0000	0.0000	0.4867(29)	1.04(3)
Y-249	847	0.2440(6)	−0.0067(8)	0.2500	0.32(2)	0.2440(6)	−0.0067(8)	0.2500	5.68(2)	0.0000	0.0000	0.4861(94)	0.98(4)
	854	0.2436(5)	−0.0077(7)	0.2500	0.39(3)	0.2436(5)	−0.0077(7)	0.2500	5.61(3)	0.0000	0.0000	0.4721(46)	1.25(4)
Y-247	853	0.2464(5)	0.0019(6)	0.2500	0.88(3)	0.2464(5)	0.0019(6)	0.2500	5.12(3)	0.0000	0.0000	0.4665(39)	1.32(4)
	845	0.2468(5)	0.0019(9)	0.2500	0.88(3)	0.2468(5)	0.0019(7)	0.2500	5.12(3)	0.0000	0.0000	0.4630(42)	1.41(4)
Y-245	846	0.2454(4)	0.0044(5)	0.2500	1.37(3)	0.2454(4)	0.0044(5)	0.2500	4.63(3)	0.0000	0.0000	0.4694(35)	1.55(3)
	871	0.2439(4)	0.0023(6)	0.2500	1.21(3)	0.2439(4)	0.0023(6)	0.2500	4.79(3)	0.0000	0.0000	0.4712(35)	1.58(6)

Specimen	PS No.	R_{wp}	RE	RB	B_0	Range (degrees 2e)
Y-220	720	13.59	9.69	3.40	0.18(5)	17–90
	730	15.41	12.79	4.54	0.10(4)	36–134
Y-249	847	18.84	11.57	3.90	0.40(9)	17–90
	854	18.80	12.78	4.01	0.33(6)	24–125
Y-247	853	17.61	12.92	3.72	0.27(6)	36–134
	845	16.44	11.63	2.52	0.60(7)	17–90
Y-245	846	14.05	11.68	2.00	0.47(6)	17–90
	871	16.19	14.87	2.75	0.23(5)	36–134

Note. For the expressions R_{wp} and RB, the I_k is the intensity assigned to the kth Bragg reflection. In the expression for RB, the "obs."—for observed—is put in quotation marks because the Bragg intensity (I_k) is rarely directly observed; instead, the $I_{k(\text{"obs."})}$ values are obtained from an allocation of total observed intensity in overlapped reflections to the individual Bragg reflections according to the ratios of intensities in the calculated patterns (see Ref. (2) for a detailed description).

N = the site occupancy factor. R_{wp} (R-weighted pattern) $= \left[\dfrac{\Sigma\, w_i(y_i(\text{obs.}) - 1/c\, y_i(\text{calc.}))^2}{\Sigma\, w_i(y_i(\text{obs.}))^2}\right]^{1/2}$

B_0 = the overall temperature factor.

R_{exp} = expected R-factor based on just counting statistics alone. RB (R-Bragg) $= \dfrac{\Sigma|I_{k(\text{"obs."})} - I_{k(\text{calc.})}|}{\Sigma\, I_{k(\text{"obs."})}}$

[a] These refinements *do not* include the simultaneous refinement of Eu(2) and Ca(2) and their site occupancy factors are a direct measure of the amount of Ca^{2+} in the Ca(2) lattice site.

the possibility existed that either the 0,0,0.47 or the 0,0,0.97 site might be preferred over the other. However, refinements in $P3$ gave no evidence of such preference, not even when there was only one S^{2-} per cell. The model finally accepted, therefore, is of a statistical distribution of S^{2-} equally between the two sites for all x.

Final refinements were all carried out in $P6_3$ with Eu^{3+} only at the Ca(2) site. The "goodness of fit" of the calculated to the observed diffraction pattern can be judged from the various R factors listed in Table II plus the graphical comparison in Fig. 1. The fits are good. Further, similar plots for the samples Y-220, Y-249, Y-247, and Y-245, which have 0, 0.35(4), 0.88(3), 1.29(9) Eu^{3+} per cell, respectively, indicated that there were no visible impurities in these samples. Comparison of the plots for samples Y-220 (no Eu^{3+}) and Y-245 in Fig. 1 display the effect that europium substitution has on

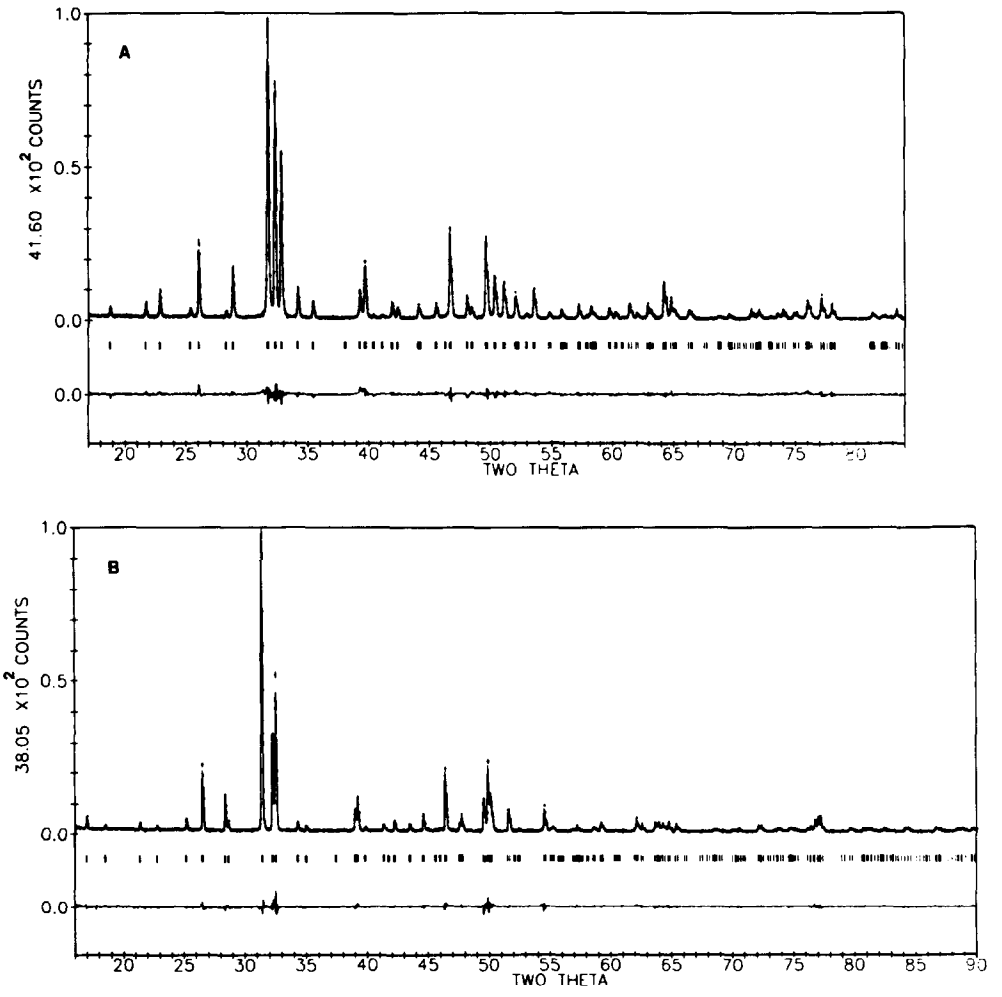

FIG. 1. Rietveld pattern fitting results for (A) Y-220 and (B) Y-245. In the upper field the points with vertical bars are the observations and the solid curve is the calculated pattern. The difference (observed minus calculated) is plotted in the lowest field. The short vertical bars in the middle field mark the positions of possible Bragg reflections for the sulfoapatite structure.

TABLE III

INTERATOMIC DISTANCES AND ANGLES CALCULATED FROM RESULTS OF TABLE II

Part A: Interatomic distances (Å in (Ca,Eu) sulfoapatites

Sample	PS No.	Ca(1a)[a]–O(1)[a]	Ca(1a)[a]–O(1)[b]	Ca(1a)[a]–O(1)[c]	Ca(1a)[a]–O(2)[d]	Ca(1a)[a]–O(2)[e]	Ca(1a)[a]–O(2)[f]	Ca(1a)[a]–O(3b)[a]
Y-220	720	2.36(2)	2.36(2)	2.36(2)	2.36(2)	2.36(2)	2.36(2)	3.12(2)
Y-220	730	2.42(1)	2.42(1)	2.42(1)	2.37(1)	2.37(1)	2.37(1)	3.05(1)
Y-249	847	2.50(3)	2.50(3)	2.50(3)	2.33(3)	2.33(3)	2.33(3)	3.16(3)
Y-249	854	2.31(4)	2.31(4)	2.31(4)	2.36(3)	2.36(3)	2.36(3)	3.07(3)
Y-247	853	2.49(4)	2.49(4)	2.49(4)	2.38(3)	2.38(3)	2.38(3)	2.94(4)
Y-247	845	2.46(5)	2.46(5)	2.46(5)	2.26(3)	2.26(3)	2.26(3)	2.90(5)
Y-245	846	2.36(3)	2.36(3)	2.36(3)	2.37(4)	2.37(4)	2.37(4)	2.82(6)
Y-245	871	2.30(3)	2.30(3)	2.30(3)	2.33(3)	2.33(3)	2.33(3)	2.68(5)
		Ca(1a)[a]–O(3b)[b]	Ca(1a)[a]–O(3b)[c]	Ca(1b)[a]–O(2)[a]	Ca(1b)[a]–O(2)[b]	Ca(1b)[a]–O(2)[c]	Ca(1b)[a]–O(3a)[a]	Ca(1b)[a]–O(3a)[b]
Y-220	720	3.12(2)	3.12(2)	2.74(2)	2.73(2)	2.73(2)	2.50(1)	2.50(1)
Y-220	730	3.05(1)	3.05(1)	2.78(2)	2.78(2)	2.78(2)	2.48(1)	2.48(1)
Y-249	847	3.16(3)	3.16(3)	2.71(3)	2.71(3)	2.71(3)	2.51(2)	2.51(2)
Y-249	854	3.07(3)	3.07(3)	2.72(3)	2.72(3)	2.72(3)	2.52(2)	2.52(2)
Y-247	853	2.94(4)	2.94(4)	2.68(3)	2.68(3)	2.69(3)	2.65(4)	2.65(4)
Y-247	845	2.90(5)	2.90(5)	2.61(3)	2.61(3)	2.61(3)	2.64(5)	2.64(5)
Y-245	846	2.82(6)	2.82(6)	2.53(4)	2.53(4)	2.53(4)	2.74(6)	2.74(6)
Y-245	871	2.68(5)	2.68(5)	2.56(3)	2.56(3)	2.56(3)	2.85(5)	2.85(5)
		Ca(1b)[a]–O(3a)[c]	Ca(1b)[a]–O(1)[d]	Ca(1b)[a]–O(1)[e]	Ca(1b)[a]–O(1)[f]	Ca(2)[a]–O(1)[c]	Ca(2)[a]–O(2)[b]	Ca(2)[a]–O(3a)[a]
Y-220	720	2.50(1)	2.38(2)	2.38(2)	2.38(2)	2.67(1)	2.34(1)	2.73(1)
Y-220	730	2.49(1)	2.32(1)	2.32(1)	2.32(1)	2.66(1)	2.31(1)	2.76(1)
Y-249	847	2.51(2)	2.25(3)	2.25(3)	2.25(3)	2.78(1)	2.38(2)	2.64(2)
Y-249	854	2.52(2)	2.38(4)	2.38(4)	2.38(4)	2.80(1)	2.41(2)	2.73(2)
Y-247	853	2.65(4)	2.34(4)	2.34(4)	2.34(4)	2.91(1)	2.32(1)	2.61(3)
Y-247	845	2.64(5)	2.40(5)	2.40(5)	2.40(5)	2.95(1)	2.40(2)	2.55(4)
Y-245	846	2.74(6)	2.46(4)	2.46(4)	2.46(4)	3.01(1)	2.42(1)	2.61(2)
Y-245	871	2.85(5)	2.47(4)	2.47(4)	2.47(4)	3.00(1)	2.44(1)	2.52(5)

		$Ca(2)^a$–$O(3a)^f$	$Ca(2)^a$–$O(3b)^b$	$Ca(2)^a$–$O(3b)^d$	$Ca(2)^a$–$S(1)^a$	$Ca(2)^a$–$S(1)^d$	$P(1)^a$–$O(1)^a$	$P(1)^a$–$O(2)^a$	$P(1)^a$–$O(3a)^a$	$P(1)^a$–$O(3b)^d$
Y-220	720	2.43(2)	2.31(1)	2.42(2)	2.87(1)	2.99(2)	1.52(1)	1.59(1)	1.43(2)	1.65(2)
Y-220	730	2.41(1)	2.26(1)	2.47(1)	2.88(1)	2.98(1)	1.54(1)	1.55(1)	1.49(2)	1.62(1)
Y-249	847	2.43(3)	2.32(2)	2.48(3)	2.85(4)	2.96(4)	1.54(2)	1.57(2)	1.49(3)	1.62(3)
Y-249	854	2.33(2)	2.37(2)	2.49(3)	2.80(2)	3.02(2)	1.52(2)	1.49(2)	1.55(3)	1.56(3)
Y-247	853	2.30(2)	2.37(3)	2.53(3)	2.77(2)	3.03(2)	1.49(2)	1.54(2)	1.57(4)	1.52(3)
Y-247	845	2.38(4)	2.32(3)	2.55(4)	2.76(2)	3.05(2)	1.49(2)	1.55(2)	1.51(4)	1.57(3)
Y-245	846	2.28(5)	2.42(4)	2.50(5)	2.77(1)	3.01(2)	1.50(2)	1.52(2)	1.64(4)	1.44(5)
Y-245	871	2.43(5)	2.34(5)	2.64(5)	2.77(1)	3.00(2)	1.52(2)	1.54(2)	1.43(5)	1.58(5)

Part B: Tetrahedral angles (degrees) for the phosphate tetrahedra in (Ca,Eu) sulfoapatites

Sample	PS No.	$O(1)^a$–$P(1)^a$–$O(2)^a$	$O(1)^a$–$P(1)^a$–$O(3a)^a$	$O(1)^a$–$P(1)^a$–$O(3b)^d$	$O(2)^a$–$P(1)^a$–$O(3a)^a$	$O(2)^a$–$P(1)^a$–$O(3b)^d$	$O(3a)^a$–$P(1)^a$–$O(3b)^d$
Y-220	720	107.6(6)	123(1)	104(1)	108.2(9)	104.5(9)	108.2(8)
Y-220	730	107.1(6)	120.4(9)	104(1)	108.3(7)	105.1(8)	111.2(7)
Y-249	847	108(1)	130(2)	95(2)	108(2)	107(2)	106(1)
Y-249	854	110(1)	118(2)	106(2)	108(1)	105(2)	108(1)
Y-247	853	110(1)	119(2)	102(2)	111(2)	106(2)	109(2)
Y-247	845	112(1)	119(3)	105(3)	110(2)	102(2)	108(2)
Y-245	846	113.3(9)	106(3)	116(3)	107(3)	106(3)	108(2)
Y-245	871	113.4(9)	110(3)	114(3)	117(2)	95(2)	108(2)

Note. The superscripts in part A refer to the atom positions in Table I translated by the following symmetry operations plus unit cell translations as needed: ^{a} x, y, z; ^{b} $\bar{y}, x-y, z$; ^{c} $y-x, \bar{x}, z$; ^{d} $\bar{x}, \bar{y}, \frac{1}{2}+z$; ^{e} $x-y, z, \frac{1}{2}+z$; ^{f} $y, y-x, \frac{1}{2}+z$. The designation of Ca(2) in this table should be interpreted as Ca^{2+} for Y-220 and a mixture of Ca^{2+} and Eu^{3+} for samples Y-245, Y-247, and Y-249.

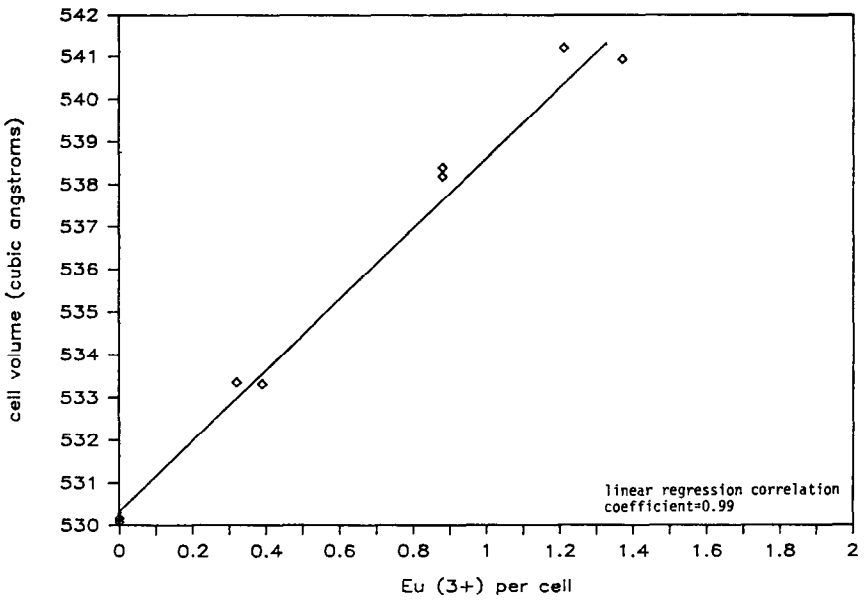

FIG. 2. A Vegard's law test with $Ca_{10-x}Eu_x(PO_4)_6S_{1+x/2}$. Site occupancies are from the Rietveld refinements.

the X-ray diffraction patterns of these apatites. Atomic coordinates, site occupancies and other numerical results from the refinements in $P6_3$ are shown in Table II. Interatomic distances and angles calculated from the results in Table II data are pre-

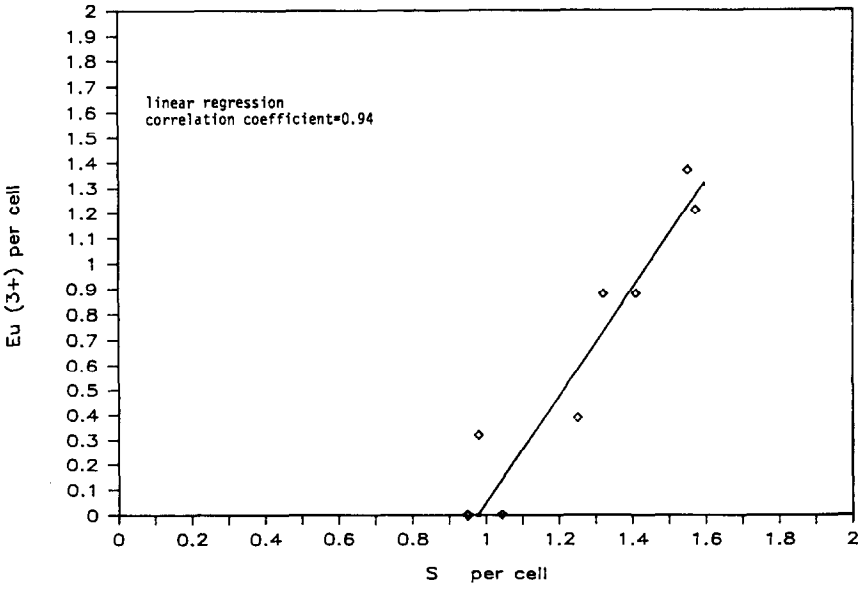

FIG. 3. Correlation of Eu and S contents in $Ca_{10-x}Eu_x(PO_4)_6S_{1+x/2}$. The site occupancies are from the Rietveld refinements.

sented in Table III. The average amount of Eu^{3+} and S^{2-} shown in Table I was determined from the average of the site occupancies obtained from the two independent data sets for each specimen.

Discussion

A plot of cell volume vs Eu^{3+} content (Fig. 2) shows that the substitution of Eu^{3+} for Ca^{2+} is continuous to at least 1.3(1) Eu^{3+} per cell; there is no indication that Eu^{3+} replaces anything else. The Eu–S content relationship (Fig. 3) shows that the substitutional mechanism for these materials was $(2Eu^{3+} + S^{2-})$ for $2Ca^{2+}$, as does the fact that Vegard's law was well obeyed when only Eu^{3+} was considered as the independent variable (Fig. 2).

As can be seen from Table III, the introduction of (Eu^{3+}, S^{2-}) for Ca^{2+} has definite structural effects. Particularly noticable are changes in various Ca–O distances and within the PO_4 tetrahedron. The structural modifications around the Ca(1) site can readily be noted through the decrease of the Ca(1a)–O(3b) and Ca(1b)–O(2) and increase of the Ca(1b)–O(3a) and Ca(1b)–O(1) interatomic distances.

Substantial changes in the various Ca,Eu(2)–O distances are also caused by the progressive substitution of Eu^{3+} for

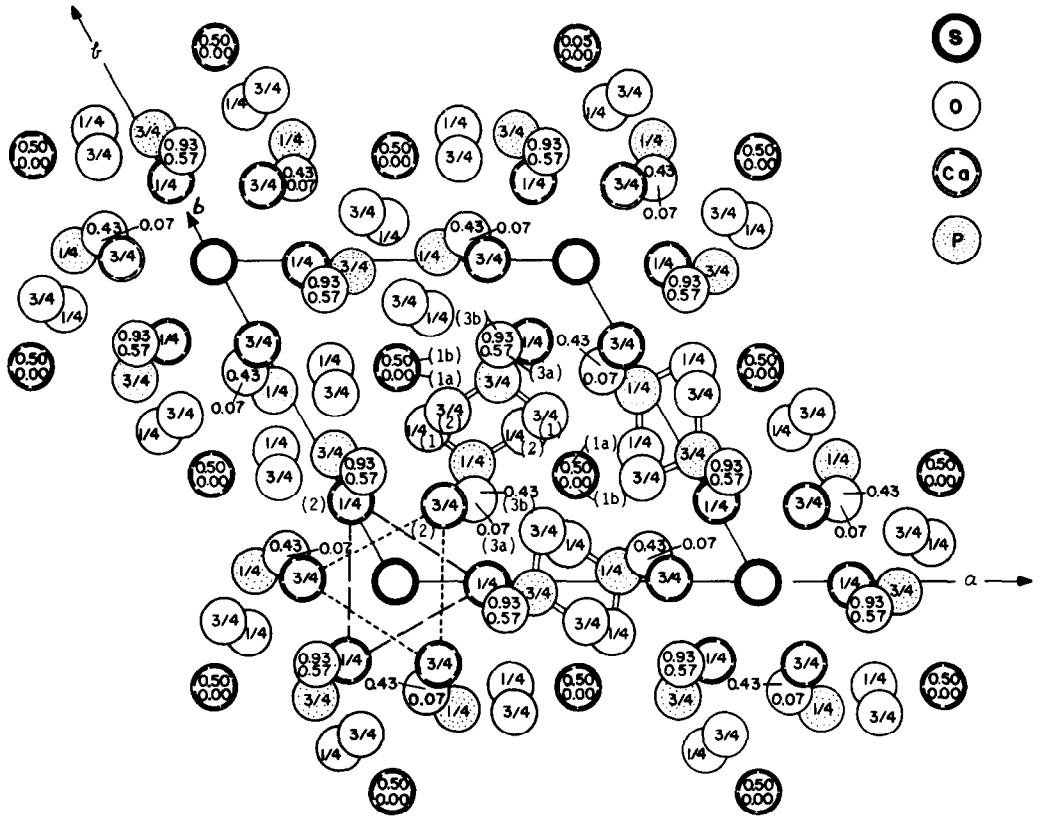

FIG. 4. The sulfoapatite structure. The atom types are classified as for space group $P6_3/m$ and the number and letters in parentheses designate the subset of the atom type in $P6_3$. The other numbers are z coordinates. S occurs at 0,0,0.47 and 0,0,97. The other ions occur essentially where they would in space group $P6_3/m$.

Ca^{2+} at the Ca(2) site (Table III). Interestingly, neither those changes nor the progressive filling of a second S^{2-} site per unit cell seems to have any significant effect on the S^{2-} positions (Table II).

The progressive changes in the Ca(1)–O distances can be visualized largely in terms of rotation of the PO_4 groups. In Table II one sees that the values for x and y increase for O(1) and O(3b) while they decrease for O(3a) with increasing Eu^{3+} for Ca^{2+} (which is accompanied by a corresponding addition of S^{2-} ions near the center of the O(3) triangles where they exert a direct influence on these O(3) ions). This motion may be thought of as a rotation of the PO_4 tetrahedron about an axis in the xy plane. This causes O(3a) to be moved toward the Ca,Eu(2) site (see Fig. 4) while O(3b) rotates toward Ca(1a). To account for the changes around the Ca,Eu(2) site, another structural change must also take place in the PO_4^{3-} groups in conjunction with the previous rotation. This involves the reshaping of the PO_4^{3-} "tetrahedron" through the scissoring of the O(1)–P(1)–O(3a) tetrahedral bond with increased incorporation of Eu^{3+} into the structure. This motion of the tetrahedron causes O(1) to move far enough away from the europium so that its Eu–O(1) bond distance is greater than 3 Å.

Conclusions

The following conclusions were drawn from this investigation.

(1) Substitution of (Eu,S) for calcium in sulfoapatite is continuous up to at least 1.3(1) and 1.6(1) atoms of Eu^{3+} and S^{2-}, respectively. The substitution takes place in the constant ratio of $2Eu^{3+}$ for each S^{2-}. Thereby charge balance is maintained and Vegard's law holds.

(2) The location of Eu^{3+} was determined by the Rietveld method to be exclusively at the Ca(2) site while S^{2-} occurred equally at 0,0,0.47 and 0,0,0.97, regardless of the S^{2-} content.

(3) The incorporation of Eu^{3+} into the sulfoapatite structure caused structural changes around both the Ca(1) sites and the Ca(2) sites which can be visualized as a combined mechanism of PO_4^{3-} tetrahedral rotation and scissoring.

Acknowledgment

This work has been supported in part by the USPHS through NINH-NIDR Grant DE-01912.

References

1. M. E. J. Curzon and T. W. Cutress, "Trace Elements and Dental Disease," John Wright, Boston (1983).
2. R. Yu Abdulsabirov and I. N. Kurkin, *Opt. Spectrosc. (Engl. Transl.)* **32,** 224 (1972).
3. A. M. Morozov, L. G. Morozova, A. K. Trefimov, and P. P. Feofilov, *Opt. Spectrosc. (Engl. transl.)* **29,** 590 (1970).
4. V. I. Kovalenko, V. S. Antipin, N. V. Vladykin, Ye. V. Smirnova, and Yu. A. Balashova, *Geochem. Int.* **19,** 171 (1982).
5. R. A. Young and J. C. Elliott, *Arch. Oral Biol.* **11,** 699 (1966).
6. J. S. Prener, *Electrochem. Soc.* **114,** 77 (1967).
7. A. W. Hounslow and G. Y. Chao, *Canad. Mineral.* **10,** 252 (1970).
8. J. C. Elliott, P. E. Mackie, and R. A. Young, *Science* **180,** 1055 (1973).
9. J. C. Elliott, G. Bonel, and J. C. Trombe, *J. Appl. Crystallogr.* **13,** 618 (1980).
10. P. R. Suitch, J. L. LaCout, A. Hewat, and R. A. Young *Acta Crystallogr. Sect. B* **41,** 173 (1985).
11. P. E. Mackie, J. C. Elliott, and R. A. Young, *Acta Crystallogr. B* **28,** 1840 (1972).
12. V. O. Khudolozhkin, V. S. Urusov, and K. I. Tobelko, *Geochem. Int.* **9,** 827 (1972).
13. V. O. Khudolozhkin, V. S. Urusov, and K. I. Tobelko, *Geochem. Int.* **10,** 1171 (1973).
14. A. Taitai, these, L'Institut National Polytechnique de Toulouse, Toulouse, France (1985).
15. A. Taitai, J. L. LaCout, and G. Bonel, *Ann. Chem. Fr.* **10,** 29 (1985).
16. A. J. C. Wilson, K. Sudarsanan, and R. A. Young, *Acta Crystallogr. Sect. B* **33,** 3142 (1977).

17. K. SUDARSANAN, R. A. YOUNG, AND A. J. C. WILSON, *Acta Crystallogr. Sect. B* **33,** 3136 (1977).
18. H. M. RIETVELD, *J. Appl. Crystallogr.* **30,** 65 (1969).
19. R. A. YOUNG AND D. B. WILES, *Adv. X-Ray Anal.* **4,** 1 (1981).
20. D. B. WILES AND R. A. YOUNG, *J. Appl. Crystallogr.* **14,** 149 (1981).
21. "International Tables for X-Ray Crystallography," Vol. IV, Kynoch Press, Birmingham (1974).
22. W. R. BUSING, K. O. MARTIN, H. A. LEVY, G. M. BROWN, C. K. JOHNSON, AND W. E. THIESSEN, *J. Appl. Crystallogr.* **6,** 309 (1979).